Sugar Recognition by the Glucose and Mannose Permeases of *Escherichia coli*. Steady-State Kinetics and Inhibition Studies†

Luis F. García-Alles,* Alain Zahn, and Bernhard Erni

Departement für Chemie und Biochemie, Universität Bern, Freiestrasse 3, CH-3012 Bern, Switzerland

Received April 5, 2002; Revised Manuscript Received June 7, 2002

ABSTRACT: The glucose (EII^{Glc}) and mannose (EII^{Man}) permeases of the phosphoenolpyruvate:sugar phosphotransferase system (PTS) of *Escherichia coli* belong to structurally different families of PTS transporters. The sugar recognition mechanism of the two transporters is compared using as inhibitors and pseudosubstrates all possible monodeoxy analogues, monodeoxyfluoro analogues, and epimers of D-glucose. The analogues were tested as phosphoryl acceptors in vitro and as uptake inhibitors with intact cells. Both EII have a high K_m of phosphorylation for glucose modified at C-4 and C-6, and these analogues also are weak inhibitors of uptake. Conversely, modifications at C-1 (and also at C-2 with EII^{Man}) were well tolerated. OH-3 is proposed to interact with hydrogen bond donors on EII^{Glc} and EII^{Man}, since only substitution by fluorine was tolerated. Glucose-6-aldehydes, which exist as *gem*-diols in aqueous solution, are potent and highly selective inhibitors of "nonvectorial" phosphorylation by EII^{Glc} (K_I 3−250 μM). These aldehydes are comparatively weak inhibitors of transport by EII^{Glc} and of phosphorylation and transport by EII^{Man}. Both transporters display biphasic kinetics (with glucose and some analogues) but simple Michaelis−Menten kinetics with 3-fluoroglucose (and other analogues). Kinetic simulations of the phosphorylation activities measured with different substrates and inhibitors indicate that two independent activities are present at the cytoplasmic side of the transporter. A working model that accounts for the kinetic data is presented.

Glucose and *N*-acetylglucosamine are the monomer building blocks of the two most abundant biopolymers, cellulose and chitin, respectively. Glucose is the preferred and sometimes unique carbon and energy source of many cells. High molecular weight polymers are hydrolyzed extracellularly by secreted enzymes, and the products are then taken up by facilitated diffusion or by ATP-powered or ion gradient-driven active transport. Eubacteria, in addition, utilize a third pathway for the uptake of carbohydrates: group translocation, a mechanism that couples translocation to phosphorylation of the solute. Group translocation of glucose is mediated by the bacterial phosphoenolpyruvate:sugar phosphotransferase system (PTS)[1] (*1*). This system consists of two cytoplasmic proteins, enzyme I (EI) and HPr, and a variable number of sugar-specific transport complexes (EII^{sugar}). The phosphoryl group of phosphoenolpyruvate (PEP) is transferred from EI to the phosphoryl carrier protein HPr and from this to the different transport complexes. In addition to transport, the PTS controls the metabolism in response to the availability of carbohydrates (*2*, *3*). PTS are ubiquitous in eubacteria but do not occur in archaebacteria and eukaryotes.

The sugar-specific transport complexes (EII^{sugar}) are homodimers as indicated by cross-linking, ultracentrifugation, gel filtration, interallelic complementation, and cryoelectron crystallography (*4*−*8*). One protomer comprises three (or four) functional units, IIA, IIB, and IIC (IID), which occur either as protein subunits or as domains in polypeptide chains. IIA and IIB sequentially transfer phosphoryl groups from HPr to the transported sugars. IIC contains the major determinants for sugar recognition and translocation, as inferred from binding studies (*9*) and the glucose selectivity of a chimeric protein between the IIC domain of EII^{Glc} and the IIA−IIB domains of the *N*-acetylglucosamine transporter (EII^{GlcNAc}) (*10*). EI, HPr, and IIA are phosphorylated at His, whereas IIB domains are phosphorylated at either Cys or His depending on the particular transporter.

Escherichia coli has two PTS transporters for glucose, EII^{Glc} (IIA^{Glc}-$IICB^{Glc}$) (*5*, *11*) and EII^{Man} ($IIAB^{Man}$-IIC^{Man}-IID^{Man}) (*12*, *13*). EII^{Glc} is a high-capacity transporter for glucose, and its expression is controlled by glucose. EII^{Man} is believed to be a scavenger for carbohydrates released during cell wall remodeling. It has a broad substrate specificity, including glucose, and is the only transporter for mannose, hence its name. Expression of EII^{Man} is nearly constitutive. Both transporters phosphorylate glucose at OH-

† This study was supported by Grant 3100-063420 from the Swiss National Science Foundation and a fellowship from the Secretaría de Estado de Educación y Universidades (Spain) to L.F.G.-A.

* To whom correspondence should be addressed. Tel: ++41-31-6313792. Fax: ++41-31-6314887. E-mail: garcia@ibc.unibe.ch.

[1] Abbreviations: PTS, phosphoenolpyruvate:sugar phosphotransferase system; EI, enzyme I of the PTS; HPr, histidine-containing phosphocarrier protein of the PTS; PEP, phosphoenolpyruvate; EII^{sugar}, sugar-specific transport complex of the PTS; $IICB^{Glc}$, transmembrane subunit of the glucose transporter; IIC^{Man}-IID^{Man}, transmembrane subunits of the mannose transporter; LDHase, L-lactate dehydrogenase; G6P, D-glucose 6-phosphate; G6PDHase, D-glucose-6-phosphate dehydrogenase; αMGlc, methyl α-D-glucopyranoside; 2dGlc, 2-deoxy-D-glucose; DTT, dithiothreitol; IC_{50}, half inhibitory concentration; TLC, thin-layer chromatography; MS (ESI), electrospray ionization mass spectrometry.

10.1021/bi025928d CCC: $22.00
Published on Web 07/09/2002

6. Despite their overlapping substrate specificity and analogous mechanism of action, EII^{Glc} and EII^{Man} belong to two different families of paralogous and orthologous transporters (for a review see ref *14*). The topology of the membrane-spanning units IIC^{Glc} and IIC^{Man}-IID^{Man} and the folds of the soluble units IIA^{Glc}, IIB^{Glc}, and $IIAB^{Man}$ are also different (*15*, *16*).

The molecular mechanism of substrate recognition and translocation by EII^{Glc} and EII^{Man} is poorly understood. Both mediate "vectorial" phosphorylation (phosphorylation coupled with transport) and "nonvectorial" phosphorylation (phosphorylation of the substrate without transport). There is evidence that nonvectorial phosphorylation occurs in intact cells when intracellular sugars are phosphorylated by EII (*17*, *18*). However, whereas the uptake of extracellular substrates and the phosphorylation of intracellular substrates by EII^{Glc} are competitive, the two activities of EII^{Man} are independent (*19*, *20*). Nonvectorial phosphorylation is assayed in vitro with membrane fractions and/or with purified EII. Vectorial phosphorylation is measured as [^{14}C]sugar uptake by intact cells.

The objective of this study was to characterize the role of the different hydroxyl groups of the pyranose ring of glucose in uptake and phosphorylation mediated by EII^{Glc} and EII^{Man}. Deoxy and fluoro analogues of glucose and its epimers were used to differentiate between potential donors and acceptors of hydrogen bonds. It is assumed that fluorine can substitute for OH groups which act exclusively as H-bond acceptors but not for those which act as H-donors. Geminal diols (aldehyde hydrates) at position C-6 were also used to characterize the reactive OH-6 group of the sugar.

EXPERIMENTAL PROCEDURES

Materials. Sugar derivatives were obtained from the following suppliers (in parentheses): D-glucose (Glc, Fluka), methyl α-D-glucopyranoside (αMGlc, Fluka), methyl α-D-mannopyranoside (αMMan, Fluka), 1,5-anhydro-D-glucitol (1dGlc, Toronto Research Chemicals), 2-deoxy-D-glucose (2dGlc, Fluka), 3-deoxy-D-glucose (3dGlc, Sigma), 4-deoxy-D-glucose (4dGlc, Chemprosa), 6-deoxy-D-glucose (6dGlc, Fluka), α-D-glucopyranosyl fluoride (α-1FGlc, Sigma), *β*-D-glucopyranosyl fluoride (*β*-1FGlc, Sigma), 2-fluoro-2-deoxy-D-glucose (2FGlc, Calbiochem), 3-fluoro-3-deoxy-D-glucose (3FGlc, Toronto Research Chemicals), 4-fluoro-4-deoxy-D-glucose (4FGlc, Apollo Chemicals), 6-fluoro-6-deoxy-D-glucose (6FGlc, Sigma), D-mannose (Fluka), D-allose (Fluka), D-galactose (Merck), 4-nitrophenyl *β*-D-glucopyranoside (*p*NFGlc, Fluka), [^{14}C]αMGlc (NEN), [^{14}C]2dGlc (Amersham). D-Glucal was obtained by deacetylation of tri-*O*-acetyl-D-glucal (Fluka) (*21*). Organic solvents were of the highest purity commercially available. Chemicals used in the synthesis of aldehydes **1a**−**f** were purchased from Fluka. Flash chromatography was done with Fluka silica gel 60/230−400 mesh. For other materials see ref *22*.

Bacterial Strains and Overproduction and Purification of Proteins. E. coli K12 ZSC112LΔ*G* (*glk manZ* Δ*ptsG:Cm*) was used as host for all experiments (*23*). Plasmid pTSGH11 encodes under the control of Ptac a $IICB^{Glc}$ with a carboxy-terminal hexahistidine tag (*6*). Plasmid pJFLPM encodes the three subunits of the *E. coli* mannose transporter under the control of the Ptac promoter (*24*). Cells were grown at 37 °C in LB medium containing appropriate antibiotics. Membranes containing $IICB^{Glc}$ and $IIAB^{Man}$/IIC^{Man}/IID^{Man}, respectively, were prepared as described (*25*). $IICB^{Glc}$ was overexpressed and purified by metal chelate affinity chromatography as published (*23*). EI, HPr, and IIA^{Glc} containing cell extracts were prepared and the proteins purified as reported (*19*).

In Vitro Phosphotransferase Assays. Pyruvate evolution from PEP upon phosphorylation of glucose analogues was measured spectrophotometrically in 96-well microtiter plates at 30 °C, using a coupled assay with L-lactate dehydrogenase (LDHase) and NADH. In inhibition studies the formation of glucose 6-phosphate (G6P) was measured in two ways: using the glucose-6-phosphate dehydrogenase (G6PDHase) coupled assay (*22*) and measuring phosphorylation of 0.45 mM radioactive [^{14}C]αMGlc or [^{14}C]2dGlc, as described (*25*). The reactions were started by addition of the sugar/inhibitor solution (20 μL) to a preincubated mixture of the rest of the components (130 μL). Final concentrations were 0.5 μM EI, 1 μM HPr, 15 μM IIA^{Glc} (or 0.5 μM $IIAB^{Man}$), 0.0013 μL/μL membrane extract, 1 mM PEP, 50 mM K_2HPO_4 buffer (pH = 7.5), 2.5 mM DTT, 2.5 mM NaF, 10 mM KCN, 5 mM $MgCl_2$, 0.25 mg/mL lecithin (Sigma), 1 unit/mL LDHase (or G6PDHase), and 0.4−0.6 mM NADH (or 1 mM NADP). Studies were carried out at rate-limiting concentrations of the transporter component. Background activities were determined in the absence of sugar and subtracted before subsequent calculations. Half inhibitory concentrations (IC_{50}) of aldehydes **1a**−**f** were determined by titration of the inhibitor (0−5 mM) in the presence of 0.1 mM D-glucose.

In Vivo Transport Inhibition. Uptake of [^{14}C]αMGlc (or [^{14}C]2dGlc) by bacteria expressing the glucose transporter (or the mannose transporter) was assayed as described (*26*). Cells were grown to saturation in 250 mL of M9 mineral medium supplemented with 0.2% glucose and 5 μM IPTG, collected by centrifugation, and resuspended in 10 mL of M9 medium without supplement. After a second step of centrifugation and resuspension in 15 mL of M9 medium, the cells were gently shaken for 10 min at room temperature and finally kept on ice. This cell suspension (0.3 mL) was diluted with 0.7 mL of M9 medium and aerated for 10 min at room temperature. Uptake was started by the addition of 10 μL of a solution containing substrate (10 mM [^{14}C]αMGlc, 4800 dpm/nmol, or [^{14}C]2dGlc, 5500 dpm/nmol) and inhibitor (100 mM). Aliquots of 100 μL were withdrawn (typically after 5, 15, 25, 40, and 120 s), diluted into 4 mL of ice-cold M9 containing 0.8 mM D-glucose, filtered through glass fiber filters (GF/F Whatman) under suction, and washed with 20 mL of ice-cold 0.15 M NaCl. The filters were dried and counted. The dry weight was determined from 0.2 mL of the concentrated cell suspension.

Fitting of Kinetic Data Using DynaFit. This software was available free of charge at http://www.biokin.com. The kinetic constants for the different steps were first estimated from the initial rates in the absence of inhibitor by fitting to the model without inhibition. Subsequently, all data measured in the presence of the inhibitor (0−15 μM for EII^{Glc} or 0−150 μM for EII^{Man}) were considered for fitting to the model accounting for inhibition. All kinetic constants were left as adjustable parameters. Figure 1 shows an example of input script file for fitting the initial velocities to model A of Figure

```
[task]
   task  = fit
   data  = velocities

[mechanism]
   E1 + S <==> E1S : Ks1 dissoc
   E1S ---> E1 + P : k1
   E2 + S <==> E2S : Ks2 dissoc
   E2S ---> E2 + P : k2
   E1 + I <==> E1I : Ki1 dissoc
   E2 + I <==> E2I : Ki2 dissoc

[constants]
  Ks1 = 100?, k1 = 500?, Ki1 = 10?
  Ks2 = 500?, k2 = 500?, Ki2 = 10?

[concentrations]
   E1 = 0.0225,   E2 = 0.0225

[responses]
   P = 1

[progress]
   rapid equilibrium

[velocity]
   directory ./inhibition_1a/data
   extension  txt
   variable   S

   file 0mM_Inh    | conc. I = 0
   file 1.7mM_Inh  | conc. I = 1.67
   file 5mM_Inh    | conc. I = 5
   file 15mM_Inh   | conc. I = 15

[output]
   directory ./inhibition_1a/output/

[settings]
   <Marquardt>
      interrupt = 500

[end]
```

FIGURE 1: DynaFit input script file for fitting the inhibition data to model A of Figure 7. E1 and E2 represent two independent enzyme activities, S is the sugar phosphoryl acceptor, P is the sugar 6-phosphate, and I is the inhibitor. Ks1 and Ks2 represent the dissociation constants, k1 and k2 the turnover rates, and Ki1 and Ki2 the inhibition constants for each enzyme activity.

7 (including inhibition). Instructions given in the reference manual of the program as well as in the literature were followed in the use of DynaFit (*27*).

Synthesis of Sugar 6-Aldehydes ***1a*****−*****f***. The selective oxidation of the primary hydroxyl group was accomplished following a described method (*28*). The polyol (D-glucose, methyl α-D-glucopyranoside, methyl α-D-mannopyranoside, *p*-nitrophenyl *β*-D-glucopyranoside, and D-glucal) (2.6 mmol) in 2.5 mL of pyridine was treated at room temperature with chlorotrimethylsilane (1.2 mequiv per OH group of the polyol). After being allowed to stand for 3 h, the mixture was diluted with 20 mL of diethyl ether and washed with 3 × 15 mL of water. The organic phase was dried over sodium sulfate, concentrated in vacuo, and flash chromatographed with hexanes−ethyl acetate (8:2) to afford the pertrimethylsilylated sugars in 65−85% yields. These derivatives (2.2 mmol) were dissolved in 3 mL of dry CH_2Cl_2 and added to a flask kept on ice and containing a suspension of finely ground chromium(VI) oxide (1.32 g) in 44 mL of dry CH_2Cl_2 and 2.1 mL of dry pyridine that had been stirred before at room temperature for 30 min. After 1 h the mixture was filtered over silica gel, and the filtrate was concentrated in vacuo. The silylated sugar 6-aldehydes were purified by flash chromatography using hexanes−ethyl acetate (8:2), unless otherwise indicated. A table with ^{1}H and ^{13}C NMR data for all of these compounds is given as Supporting Information. *1,2,3,4-Tetrakis-O-(trimethylsilyl)-*D*-gluco-hexodialdo-1,5-pyranose*: 0.39 g, 40%. *Methyl 2,3,4-tris-O-(trimethylsilyl)-*α*-*D*-gluco-hexodialdo-1,5-pyranoside*: 0.37 g, 43%. *Methyl 2,3,4-tris-O-(trimethylsilyl)-*α*-*D*-manno-hexodialdo-1,5-pyranoside*: 0.15 g, 17%. *4-Nitrophenyl 2,3,4-tris-O-(trimethylsilyl)-β-*D*-gluco-hexodialdo-1,5-pyranoside*: 0.28 g, 25%. *2,6-Anhydro-5-deoxy-3,4-bis-O-(trimethylsilyl)-*D*-lyxo-hex-5-enose*: purified using hexanes−AcOEt (92:8), 0.19 g, 31%. Also present is 30% of a side product, presumably the 1,2-dideoxy-4,6-bis-*O*-(trimethylsilyl)-D-*erythro*-hex-1-enopyranos-3-ulose.

The sugar 6-aldehydes **1a**−**e** were obtained after removal of the trimethylsilyl protecting groups from the previous derivatives (1 mmol) by stirring at room temperature with potassium carbonate (8 mg) in 8 mL of methanol. Reactions were monitored by thin-layer chromatography (TLC). After disappearance of all starting material (typically 1−3 h) the reaction mixture was cooled on ice, and the suspension was filtered off.

D-*Gluco-hexodialdo-1,5-pyranose* ***(1a)***: 120 mg, 72%. The ^{1}H and ^{13}C NMR spectra of this compound are too complex to be described. MS (ESI) *m*/*z* 201 ([M + Na]$^+$, 65%), 379 ([M + M + Na]$^+$, 100%) (*29*).

Methyl α-D-*gluco-hexodialdo-1,5-pyranoside* ***(1b)***: 180 mg, 94%; ^{1}H NMR (D_2O) *δ* 5.08 (1H, d, *J* = 1.8 Hz), 4.66 (overlapped with water signal), 3.42 (1H, q, *J* = 9.2 Hz), 3.35−3.22 (3H, m), 3.18 (3H, s, CH_3O); ^{13}C NMR (D_2O) *δ* 100.3, 89.0, 74.0, 73.4, 72.1, 71.3, 56.1 (*30*). MS (ESI) *m*/*z* 249 ([M + H_2O + K]$^+$, 45%), 423 ([M + M + K]$^+$, 100%).

Methyl α-D-*manno-hexodialdo-1,5-pyranoside* ***(1c)***: 151 mg, 79%; ^{1}H NMR (D_2O) *δ* 5.15 (1H, d, *J* = 2.2 Hz), 4.72 (overlapped with water signal), 3.72 (1H, dd, *J* = 2.6, 1.8 Hz), 3.55 (2H, m), 3.34 (1H, m), 3.21 (3H, s, CH_3O); ^{13}C NMR (D_2O) *δ* 102.0, 89.3, 74.3, 71.4, 70.8, 68.2, 55.8. MS (ESI) *m*/*z* 233 ([M + H_2O + Na]$^+$, 100%).

*p-Nitrophenyl β-*D*-gluco-hexodialdo-1,5-pyranoside* ***(1d)***: purified by flash chromatography using AcOEt−MeOH (96:4), 167 mg, 56%; ^{1}H NMR (D_2O) *δ* 8.08 (2H, d, *J* = 9.2 Hz, ArH), 7.09 (2H, d, *J* = 9.2 Hz, ArH), 5.17 (1H, s), 5.09 (1H, m), 3.50 (4H, br); ^{13}C NMR (D_2O) *δ* 162.1, 142.9, 126.4, 116.9, 100.1, 88.3, 77.1, 75.6, 72.9, 70.3. MS (ESI, solubilized in MeOH) *m*/*z* 354 ([M + MeOH + Na]$^+$, 50%), 685 ([(M + MeOH)$_2$ + Na]$^+$, 100%).

*2,6-Anhydro-5-deoxy-*D*-lyxo-hex-5-enose* ***(1e)***: obtained after being stirred for 3 h at room temperature 1 mmol of the 3,4-bis-*O*-(trimethylsilyl) derivative in 12 mL of H_2O−MeOH (1:1) and lyophilization; 0.138 mg, 96%; ^{1}H NMR (D_2O) *δ* 6.31 (1H, dd, *J* = 6.2, 1.5 Hz, H1), 5.22 (1H, d, *J* = 2.9 Hz, H6), 4.73 (1H, dd, *J* = 6.2, 2.6 Hz, H2), 4.11 (1H, dt, *J* = 6.6, 2.2 Hz), 3.71−3.56 (2H, m); ^{13}C NMR (D_2O) *δ* 143.9, 103.0, 87.5, 79.1, 69.4, 68.1. MS (ESI) *m*/*z* 167 ([M + Na]$^+$, 10%), 311 ([M + M + Na]$^+$, 60%). Around 30% of presumably 1,2-dideoxy-D-*erythro*-hex-1-enopyranos-3-ulose was also present: ^{1}H NMR (D_2O) *δ* 7.48 (1H, d, *J* = 5.5 Hz), 5.36 (1H, d, *J* = 5.5 Hz), 4.38 (1H, d, *J* = 13.2 Hz), 4.23 (1H, ddd, *J* = 13.2, 4.4, 2.2 Hz), 3.91−3.72 (2H, m); ^{13}C NMR (D_2O) *δ* 166.1, 104.0, 94.7, 82.8, 78.2, 60.3.

*Methyl 4-deoxy-β-*L*-threo-hex-4-enodialdo-1,5-pyranoside* ***(1f)***: obtained from **1b** as described (*31*). Preparative TLC was eluted with AcOEt−MeOH (92:8). ^{1}H NMR (acetone-d_6) *δ* 9.23 (1H, s, H6), 5.93 (1H, d, *J* = 2.9 Hz, H4), 4.94 (1H, d, *J* = 2.6 Hz, H3), 4.56 (1H, br), 4.38 (1H, br), 4.26 (1H, br), 3.68 (1H, br), 3.40 (3H, s, CH_3O); ^{13}C NMR (acetone-d_6) *δ* 188.1, 150.3, 125.0, 103.0, 72.9, 68.1, 57.7. MS (ESI) *m*/*z* 197 ([M + Na]$^+$, 60%), 371 ([M + M + Na]$^+$, 100%).

RESULTS

Epimers and Deoxy and Fluoro Analogues of D-*Glucose*. Mannose, allose, galactose, five monodeoxy analogues, and six monofluoro analogues with the same stereochemistry as glucose were assayed in vitro as substrates of EII^{Glc} and EII^{Man}. Phosphotransferase activity was monitored by reduction of the pyruvate evolved from PEP in the presence of LDHase. Disappearance of NADH was recorded continuously. Initial rates measured in the presence of rate-limiting amounts of EII^{Glc} or EII^{Man} as a function of the sugar concentration were fitted to a Michaelis−Menten hyperbola (plots are furnished as Supporting Information). The catalytic

Table 1: Kinetic Constants for the Phosphorylation of Epimers and Deoxy and Deoxyfluoro Analogues of D-Glucose by the Glucose and the Mannose Transporters of *E. coli*[a]

	EII^{Glc}				EII^{Man}			
sugar	V_{max}[b]	K_m[c]	V_{max}/K_m[d]	% Glc[e]	V_{max}[b]	K_m[c]	V_{max}/K_m[d]	% Glc[e]
Glc	43	0.22	200	100	36	0.49	72	100
1dGlc	47	0.20	240	119	34	1.1	31	42
α-1FGlc	41	0.21	190	98	28	0.48	57	79
β-1FGlc	42	0.19	220	112	35	0.47	74	102
mannose	50	4.8	10	5	39	0.32	120	169
2dGlc	51	1.5	34	17	43	0.49	87	120
2FGlc	43	1.2	36	18	39	0.45	87	120
allose	ND[f]	>8	6.8	3	ND	>9	6.4	9
3dGlc	65	4.1	16	8	50	2.0	25	34
3FGlc	51	0.49	105	53	40	0.61	66	91
galactose	ND	ND	1.0	0.5	ND	ND	0.6	1
4dGlc	16	4	4.4	2	ND	ND	0.2	0.3
4FGlc	25	1.7	15	7	18	5	3.6	5
6dGlc	ND	ND	<0.05	<0.02	ND	ND	<0.05	<0.1
6FGlc	ND	ND	<0.05	<0.02	ND	ND	<0.05	<0.1

[a] Phosphorylation was measured at 30 °C with the LDHase coupled assay (Experimental Procedures). Kinetic constants were derived from a best fit to a Michaelis−Menten hyperbola. [b] Units: μM min^{-1} using 0.0013 μL/μL of membrane extract. The standard deviation is <6%, except for 4dGlc with EII^{Glc} which was 25%. [c] Units: mM. Standard errors vary between 5% and 16%, except for 4dGlc with EII^{Glc} where it is 40%. [d] Units: min^{-1} × 10^3 using 0.0013 μL/μL of membrane extract. Standard errors vary between 6% and 22%, except for 4dGlc with EII^{Glc} where it is 65%. [e] 100(V_{max}/K_m)/[V_{max}(Glc)/K_m(Glc)]. [f] ND: could not be determined.

constants obtained by nonlinear regression from these progress curves are summarized in Table 1.

EII^{Glc} tolerates all fluoro and deoxy modifications at C-1. Inversion or replacement of OH-2 increases the K_m of EII^{Glc} 6−20-fold but does not affect V_{max}. Modifications at C-3 are of special interest. Inversion of the OH and replacement by H increase the K_m of EII^{Glc} by more than 20-fold, whereas replacement by F has almost no effect, indicating that OH-3 might function as a H-bond acceptor. Modifications at C-4 are not tolerated. They increase K_m of EII^{Glc} 10−20-fold and decrease V_{max} 3-fold. Analogues of glucose modified at C-6, the position of phosphorylation, are not substrates and only weak inhibitors. The half inhibitory concentrations (IC_{50}) measured for 6dGlc and 6FGlc in the presence of 0.1 mM glucose were approximately 4−5 mM (results not shown), indicating that OH-6 is not only chemically reactive but also an important determinant for binding.

Both EII^{Glc} and EII^{Man} accept glucose but differ in structure and mechanism of action. Do they differ with respect to which hydroxyl groups they recognize? For this comparison the catalytic constants of EII^{Man} for the same analogues were determined. Results are summarized in Table 1 (see also Supporting Information). Replacement of OH-1 by H increases K_m by a factor of 2 but does not affect significantly V_{max}. Fluorine in the α-anomeric position has little and in β has no effect. Relative to glucose, EII^{Man} has an increased V_{max} and decreased K_m for analogues modified at C-2 in the order Man > 2dGlc = 2FGlc. Taken together, these data indicate that EII^{Man} tolerates deletions and isosteric substitutions at C-1 and C-2. As with EII^{Glc}, F instead of OH at C-3 is well tolerated, but replacement by H and inversion of the OH are not, suggesting that this OH-3 plays a similar role in binding to EII^{Man} and EII^{Glc}. Also similarly to EII^{Glc},

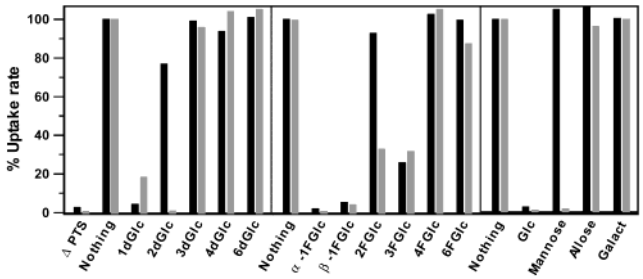

FIGURE 2: Inhibition of sugar uptake into whole cells. EII^{Glc}-dependent uptake of 0.1 mM [^{14}C]αMGlc (black bars) and EII^{Man}-dependent uptake of 0.1 mM [^{14}C]2dGlc (gray bars) in the presence of the indicated substrate analogue at a constant concentration of 1 mM. ΔPTS: background of uptake by a mutant *E. coli* lacking both EII^{Glc} and EII^{Man}. 100% uptake corresponds approximately to 20 nmol min^{-1} mg^{-1} dry weight of cells expressing EII^{Glc}, and 15 nmol min^{-1} mg^{-1} of cells expressing EII^{Man}.

Chart 1

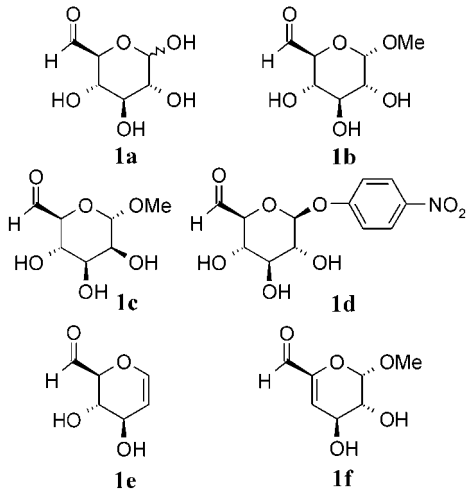

modifications at C-4 are not tolerated, and analogues modified at C-6 do not inhibit phosphorylation of 0.1 mM glucose by EII^{Man} (IC_{50} > 5 mM, not shown).

The effect of the analogues on uptake had to be assayed indirectly because radiolabeled forms for direct measurement were not available. Instead, inhibition of [^{14}C]methyl α-D-glucopyranoside (αMGlc) and [^{14}C]-2-deoxy-D-glucose (2dGlc) uptake by intact cells was measured (Figure 2). Uptake was started by the simultaneous addition of the analogue and ^{14}C-labeled substrate in a molar ratio of 10:1 to *E. coli* expressing only EII^{Glc} or EII^{Man}. The glucose analogues modified at C-1 inhibit uptake by EII^{Glc} and EII^{Man}. Analogues modified at C-2 strongly inhibit EII^{Man} and weakly inhibit EII^{Glc}. 3FGlc inhibits uptake by both transporters while the C-3 epimer allose and 3dGlc do not. When cells were preincubated for 1 min with 0.3−0.1 mM inhibitor (at which concentration uptake of simultaneously added ^{14}C-labeled sugar is not blocked), the uptake of subsequently added ^{14}C-labeled sugar (0.1 mM) was completely blocked (results not shown). This also occurs if cells are preincubated first with low concentrations of unlabeled glucose and then challenged with radiolabeled glucose. Inhibition after a short burst of uptake is attributed to the accumulation of nonmetabolizable sugar phosphates. That such inhibition is observed with analogues indicates that they are rapidly translocated into the cell.

Synthesis and Evaluation of Glucose-6-aldehydes. The OH-6 of the pyranose ring of the sugar is the reactive group

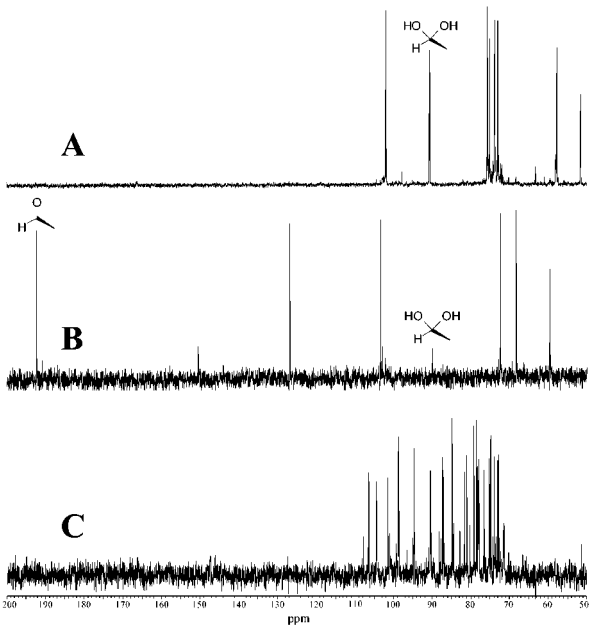

FIGURE 3: ^{13}C NMR spectra of aldehydes **1b** (A), **1f** (B), and **1a** (C) in D_2O. The diagnostically relevant signals are labeled.

Table 2: Glucose-6-aldehydes **1a**−**f** as Inhibitors of D-Glucose Phosphorylation[a]

	EII^{Glc}		EII^{Man}	
inhibitor	IC_{50} (mM)	K_I (mM)	IC_{50} (mM)	K_I (mM)
1a	0.002[b]	0.003	0.14	0.10
Glc		0.18[c]		0.13[c]
1b	0.009[b]	0.009	>5	
αMGlc	0.6[d]	0.75[d]	>5	
1c	>5		>5	
αMMan	>5		>5	
1d	0.25[b]		>5	
*p*NFGlc	2[b]		>5	
1e	4		>5	
glucal	>5[d]		>5	
1f	>5		>5	

[a] For IC_{50} determination: phosphorylation of 0.1 mM D-glucose was measured at 30 °C in the presence of 0−5 mM inhibitor, using the LDHase and the G6PDHase coupled assays. Inhibition constants were determined from experiments carried out under similar conditions, varying the concentration of D-glucose (0−2 mM) at four fixed concentrations of the inhibitor. K_I values were obtained by linear regression fit to $K_m(app) = K_m(1 + [I]/K_I)$. [b] Similar value was determined by measuring inhibition of phosphorylation of 0.45 mM [^{14}C]αMGlc. [c] K_m value. [d] Phosphorylation of the inhibitor was detected with the LDHase assay. For that reason, inhibition was measured with the G6PDHase assay.

which is phosphorylated by EII. Would an analogue with two geminal hydroxyl groups at C-6, instead of one, be recognized by EII^{Glc} and EII^{Man}? Would it be transported and/or phosphorylated? And if so, would the phosphoryl hemiacetal hydrolyze spontaneously, as previously reported for analogous compounds (*32*−*34*), and would this reaction uncouple the phosphotransferase system and result in unchecked consumption of PEP? With this idea in mind, six glucose-6-aldehyde analogues (**1a**−**f**, Chart 1) were prepared by selective oxidation of the primary alcohol groups, following a described procedure (*28*). The ^{13}C NMR spectra confirmed that compounds **1b**−**e** are present as hydrated aldehydes in D_2O (Figure 3). The characteristic carbonyl signal at 200 ppm is absent, and a new signal emerges at 90

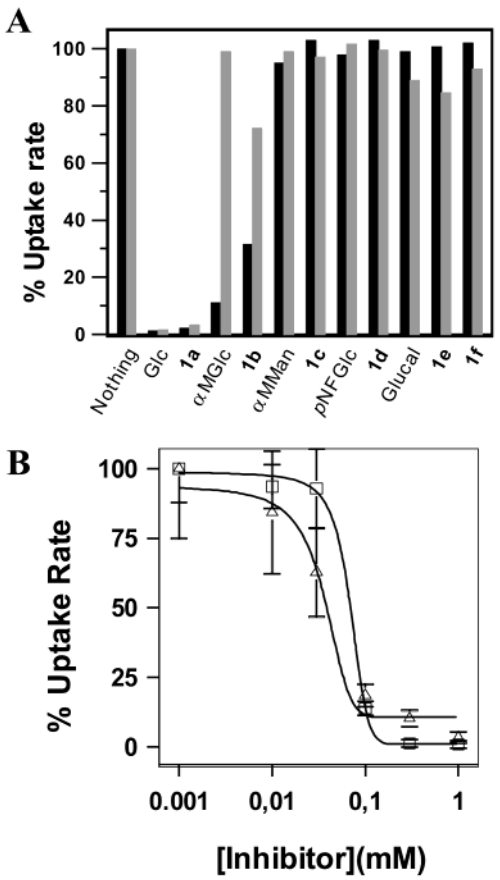

FIGURE 4: Glucose-6-aldehydes **1a**−**f** as inhibitors of sugar uptake. (A) EII^{Glc}-dependent uptake of 0.1 mM [^{14}C]αMGlc (black bars) and EII^{Man}-dependent uptake of 0.1 mM [^{14}C]2dGlc (gray bars) in the presence of the indicated glucose-6-aldehyde **1a**−**f** or the corresponding glucose-6-alcohol at a constant concentration of 1 mM. For other details see legend to Figure 2. (B) Dose−response curve: inhibition of EII^{Glc}-dependent uptake of 0.1 mM [^{14}C]αMGlc by the glucose-6-aldehyde **1a** (triangles) and glucose (squares).

ppm. Only the α,β-unsaturated aldehyde **1f** (Figure 3B) presents a signal at 192 ppm, indicating that around 90% of this compound is in the carbonylic form. The ^1H and ^{13}C NMR spectra of **1a** were complex, indicating that this 1,6-dialdehyde exists as an equilibrium mixture of isomers.

The glucose-6-aldehydes **1a**−**f** failed to elicit pyruvate formation in the in vitro phosphotransferase assay. Therefore, these compounds are neither substrates nor uncouplers of EII^{Glc} and EII^{Man}. However, the glucose-6-aldehyde **1a** and the methyl α-D-glucopyranoside-6-aldehyde **1b** are strong reversible inhibitors of nonvectorial phophorylation by EII^{Glc} (Table 2). The inhibition constants (K_I) were 3 μM and 9 μM, respectively. These values are remarkably low in comparison with a $K_m = 180$ μM of EII^{Glc} for D-glucose and the $K_I = 750$ μM of αMGlc determined under the same experimental conditions. Similar values were obtained in all three assays (detection of pyruvate with LDHase or G6P with G6PDHase and determination of [^{14}C]G6P). EII^{Man} is much less inhibited by the glucose-6-aldehydes than EII^{Glc}. Compound **1b** does not inhibit this transporter. The K_I of **1a** for EII^{Man} is 100 μM, 35-fold higher than for EII^{Glc} (Table 2).

Notice that **1a** is a mixture of isomers of which only one or a few might be inhibitory, and therefore the experimentally determined K_I values of 3 μM and 100 μM might be underestimated. Of the two possible pyranose isomers of **1a**,

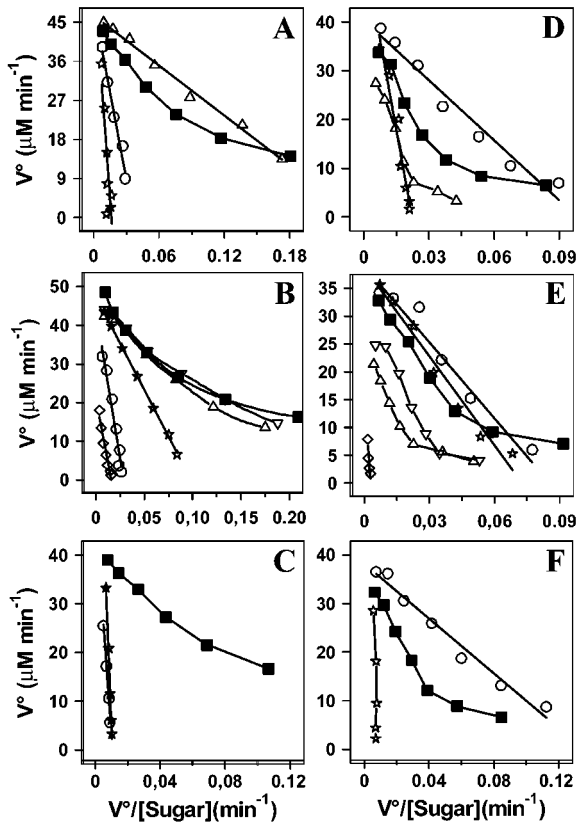

FIGURE 5: Eadie−Hofstee plots for the phosphorylation of deoxy and fluoro analogues and epimers of D-glucose: EII^{Glc} activity (A−C); EII^{Man} activity (D−F). The substrates were monodeoxy (A, D) and monodeoxyfluoro analogues (B, E) and epimers (C, F) of D-glucose at concentrations between 0 and 5 mM. Key: D-Glucose (solid squares), glucose analogue modified at C-1 [up triangles, except for β-1FGlc (down triangles)], C-2 (circles), C-3 (stars), and C-4 (diamonds). Sugar phosphorylation was measured in a coupled assay by reduction of pyruvate with LDHase. Membrane fractions were used. Two or more independent measurements were done with similar qualitative results.

the 1,5-form is expected to be more stable (all OH equatorial) than the 2,6-form (two OH axial), but its effective concentration is not known. On the other hand, the strong inhibition of EII^{Glc} by **1a** and **1b** is fully reversible, and there is no evidence for Schiff base formation between the aldehyde and essential ϵ-amino groups of the transporter. The addition of $NaBH_4$ has no effect at saturating concentrations of the glucose-6-aldehydes. Irreversible inhibition by **1a** and **1b** is only observed at excessively high concentrations (100 mM). At these concentrations inactivation is nonspecific since it is also induced with similar concentrations of formaldehyde (results not shown).

The glucose-6-aldehyde **1a** and to a lesser extent **1b** inhibit EII^{Glc}-mediated uptake of [^{14}C]αMGlc (Figure 4A). The aldehyde **1a** has an IC_{50} for uptake of 35 ± 6 μM, which is comparable to the $IC_{50} = 69 \pm 3$ μM of glucose, which is a competitive substrate of [^{14}C]αMGlc (Figure 4B). Preincubation of the cells with low concentrations of the glucose-6-aldehydes does not block subsequent uptake of [^{14}C]αMGlc (results not shown).

With its high affinity and selectivity for EII^{Glc}, the aldehydes **1a**,**b** might serve as starting compounds for the synthesis of EII^{Glc}-specific affinity and fluorescent probes. In this sense instructive is the comparison of 4-nitrophenyl

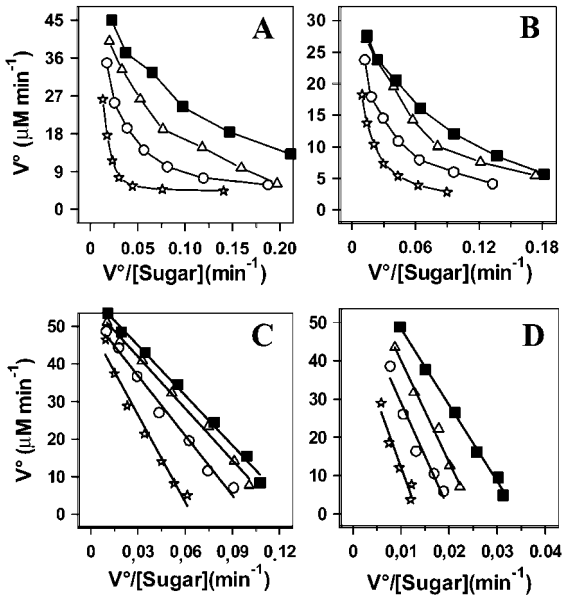

FIGURE 6: Glucose-6-aldehyde **1b** as the reversible inhibitor of EII^{Glc}. Eadie−Hofstee plots of nonvectorial phosphorylation by a EII^{Glc}-containing membrane fraction (A, C, D) and by purified EII^{Glc} (B). The substrates (phosphoryl acceptors) were D-glucose (A, B), 3FGlc (C), and 2FGlc (D). The substrate concentration [sugar] was varied between 0 and 2 mM. The inhibitor concentrations were 0 μM (squares), 1.7 μM (triangles), 5 μM (circles), and 15 μM (stars).

β-D-glucopyranoside (*p*NFGlc) and its 6-aldehyde analogue **1d** (Table 2). The 6-aldehyde inhibits nonvectorial phosphorylation of glucose by EII^{Glc} with an IC_{50} of 250 μM, whereas *p*NFGlc (which is not phosphorylated by EII^{Glc}) has an IC_{50} of 2 mM. The IC_{50} of **1d** is still lower than the IC_{50} of αMGlc, which is used as a nonmetabolizable analogue of glucose. The presence of the 6-aldehyde group seems to be beneficial for binding to EII^{Glc}. However, it is not able to compensate for more severe structural modifications such as the presence of 1,2 or 4,5 carbon−carbon double bonds in the pyranose ring (compounds **1e** and **1f**). Although a stronger inhibitor of nonvectorial phosphorylation than αMGlc, **1d** does not inhibit uptake of radioactive αMGlc mediated by EII^{Glc} (Figure 4A).

Biphasic Kinetics. When the data used to derive the kinetic constants of Table 1 are plotted in the Eadie−Hofstee form, the graphs are not always linear, as would be expected of a simple Michaelis−Menten mechanism (Figure 5). Nonlinearity is strongest with glucose and analogues modified at C-1. In contrast, data points obtained from analogues modified at C-2 or C-3 are linearly distributed. Nonlinear plots were obtained with Glc as substrate of EII^{Glc}- and EII^{Man}-containing membranes, as well as purified EII^{Glc}, and in the presence of inhibitors (Figure 6A,B). In contrast, kinetics with 2FGlc and 3FGlc as substrates afforded linear plots under all conditions (Figure 6C,D). With FGlc as substrates, inhibiton of EII^{Glc} by **1b** is competitive with K_I of 11 μM. This value is similar to the inhibition constant measured using Glc (Table 2) and therefore indicates that phosphorylation of all substrates is inhibited at the same site. Moreover, inspection of the nonlinear plots (Figure 6A,B) shows that inhibition by the aldehydes is stronger at high glucose concentrations (steep branch of the plot, low-affinity regime) than at low concentrations (shallow branch, high-affinity regime). Inhibition of EII^{Man} by **1a** also shows

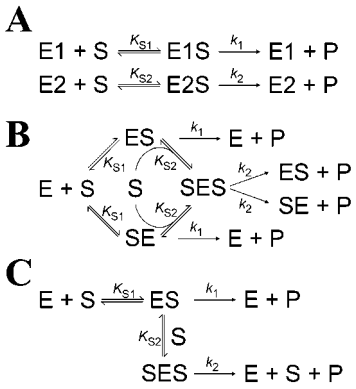

FIGURE 7: Kinetic models leading to biphasic Eadie−Hofstee plots: (A) two independent enzymes or active sites with different affinities for S, (B) two-site enzyme with two anticooperative sites, and (C) an enzyme with a catalytic and a regulatory site. In all cases $K_{S2} > K_{S1}$. ES and SE in model B represent equal forms of the singly occupied enzyme.

nonlinear plots with Glc as substrate and linear plots with 3FGlc and mannose (not shown).

Mechanism of Nonvectorial Phosphorylation. Concave Eadie−Hofstee plots, as observed with Glc as substrate of EII^{Glc} or EII^{Man}, can be explained by different kinetic models (Figure 7): (A) One enzyme with two independent active sites and different catalytic constants, a mixture of two different enzymes, or a heterogeneous preparation of one enzyme, (B) one enzyme with two anticooperative binding sites, (C) one enzyme with a catalytic and a regulatory site for the same substrate, or (D) a slow equilibrium random bi-bi reaction (with, for instance, phospho-IIA^{Glc} and Glc as the two substrates of $IICB^{Glc}$). Models A−D are represented by similar velocity equations (*35*) and therefore cannot be distinguished by enzyme/substrate kinetics alone. Additional nonkinetic criteria are required. Model D can be rejected because different substrates which are phosphorylated with similar rates, such as Glc and FGlc, should produce similar plots. A mixture of two enzymes in the membranes or heterogeneity of EII^{Glc} and EII^{Man} can be excluded as the cause, because the biphasic behavior does not change with purification. Models B and C predict a transition from a high-affinity to low-affinity state with increasing substrate concentration. Since the inhibition experiments with **1b** indicate that 2FGlc and 3FGlc are phosphorylated in the low-affinity site of EII^{Glc}, they should bind to the high-affinity site first. Consequently, they would ultimately lead to biphasic curves. Yet, the shape of the plots is linear.

The remaining model A (Figure 7) is based on two different, independent active sites. Using the program DynaFit (*27*) all the inhibition data presented in Figure 6A,B and Figure 8 were fitted to this model, including inhibition of both sites (formation of E1I and E2I). Two representative fits for inhibition of EII^{Glc} and EII^{Man} by aldehyde **1a** are shown in Figure 8A,B. For comparison, also shown is a low-quality fit of the same EII^{Man} data to the alternative model B allowing formation of EI and IES (identical to SEI) (Figure 8C). The kinetic constants from the best fit are listed in Table 3. The substrate dissociation constants (K_{S1} and K_{S2}) for the two binding sites of EII^{Glc} differ by a factor of 50, whereas the inhibition constants (K_{I1} and K_{I2}) are very similar. This means that the inhibitor competes 50 times more efficiently for binding to the low-affinity than to the high-affinity site of EII^{Glc}. Qualitatively similar results are obtained with EII^{Man}. The inhibitor binds 20 times more strongly than the substrate to the low-affinity site, whereas it binds 3 times less strongly than the substrate to the high-affinity site. The EII^{Glc} data would fit to models B and C (not shown) as well as to model A (Figure 8A). However, the EII^{Man} data fit better to model A than to model B (compare residuals of Figure 8, panels B and C) and model C (not shown). Assuming that the similarity of the data obtained with EII^{Glc} and EII^{Man}

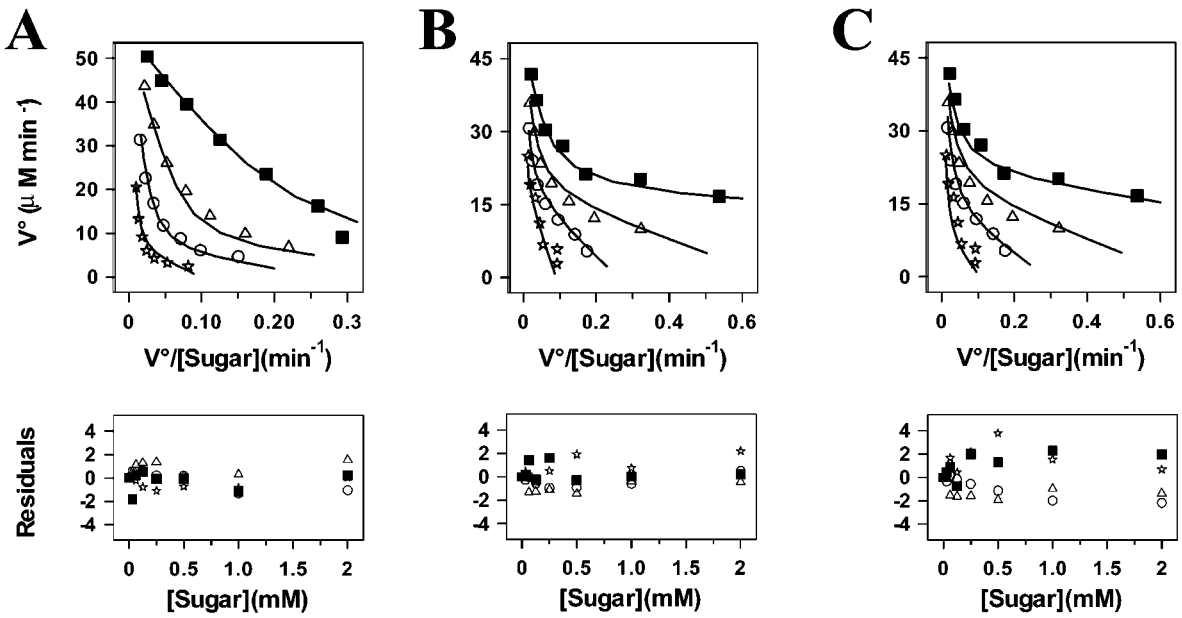

FIGURE 8: Global least-squares fit (DynaFit) of inhibition data to kinetic model A of Figure 7. Experimental data (symbols): inhibition by **1a** of glucose phosphorylation catalyzed by purified $IICB^{Glc}$ (A) or membrane fractions containing IIC^{Man}-IID^{Man} (B, C). Binding of the inhibitor to both E1 and E2 was allowed. The values of the kinetic constants resulting from the fit are given in Table 3. (C) For comparison the experimental data used in (B) were fitted to model B of Figure 7. Residuals are plotted as a function of the substrate concentration. Inhibitor concentrations were (A) 0 μM (squares), 1.7 μM (triangles), 5 μM (circles), and 15 μM (stars) and (B, C) 0 μM (squares), 17 μM (triangles), 50 μM (circles), and 150 μM (stars). All other experimental conditions were as indicated in the legend to Figure 6.

Table 3: Kinetic Constants Derived by Least-Squares Fit (DynaFit) of Inhibition Data[a]

substrate	inhibitor	K_{S1} (μM)	k_1 (s^{-1})	K_{I1} (μM)	K_{S2} (μM)	k_2 (s^{-1})	K_{I2} (μM)
				EII^{Glc} [b]			
Glc[c]	**1a**	5 ± 7	4.3 ± 0.9	1 ± 2	230 ± 20	37 ± 1	0.78 ± 0.06
Glc[c,d]	**1b**	15 ± 5	9 ± 1	5 ± 2	370 ± 42	37 ± 1	3.1 ± 0.2
Glc[d]	**1b**	9 ± 10	4 ± 1	9 ± 13	310 ± 40	37 ± 1	1.9 ± 0.2
3FGlc[e]	**1b**				380 ± 10	29 ± 1	8.5 ± 0.6
2FGlc[e]	**1b**				1900 ± 100	28 ± 2	6.4 ± 0.5
2dGlc[e]	**1b**				8000 ± 2000	47 ± 10	10 ± 2
				EII^{Man} [f]			
Glc	**1a**	19 ± 5	8.3 ± 0.8	60 ± 20	210 ± 20	20 ± 1	12 ± 1
3FGlc[e]	**1a**				300 ± 20	31 ± 1	6.2 ± 0.4
Man[e]	**1a**				140 ± 10	40 ± 1	11 ± 1

[a] Data of inhibition of EII^{Glc}- and EII^{Man}-mediated phosphorylation of the indicated substrates by aldehydes **1a** and **1b** were fitted to model A of Figure 7, including competitive inhibition of E1 and E2. The concentrations of E1 and E2 were set to be equal. Protein concentrations were estimated by Lowry. The concentration of EII^{Glc} in membranes was adjusted so as to give the same k_2 constant with glucose as substrate (lane 3) as purified IICB^{Glc} (lane 2). Accordingly, 15% of the total protein content of the membrane would correspond to IICB^{Glc}. The same proportion was supposed for IICD^{Man}-containing membranes. [b] Data measured in the presence of 0−15 μM concentrations of inhibitor, as indicated in Figure 6. [c] Data obtained with purified IICB^{Glc} instead of IICB^{Glc}-containing membrane fractions. [d] Similar fit using model A including competitive inhibition of only E2. [e] Data fitted to a simple Michaelis−Menten model with competitive inhibition. [f] Data measured in the presence of 0−150 μM inhibitor, as in Figure 8B,C.

reflects a common mechanism for both transporters, model A, two indepedent active sites per EII dimer, is the only model which can account for both linear kinetics observed with FGlc and biphasic kinetics observed with Glc.

DISCUSSION

Two classes of compounds, pseudosubstrates and inhibitors, were used to compare structural and kinetic properties of the glucose transporters EII^{Glc} and EII^{Man} and to identify minimally disruptive positions on glucose for the future synthesis of fluorescence and affinity-labeling analogues. The pseudosubstrates, namely, epimers and deoxy and fluoro analogues of glucose, can be grouped according to two criteria: (i) whether they are transport inhibitors and (ii) whether in vitro phosphorylation by EII follows simple Michaelis−Menten kinetics (linear Eadie−Hofstee plot) or not (Table 4).

Inhibition of sugar import into cells and nonvectorial phosphorylation of pseudosubstrates by EII are correlated (Figure 9). Compounds with K_m < 0.6 in nonvectorial phosphorylation are good inhibitors of transport. Substrate analogues for which the K_m of EII^{Glc} or EII^{Man} is larger than 1.6 mM do not interfere with [^{14}C]αMGlc or [^{14}C]2dGlc uptake. This correlation suggests that the OH groups of the substrate interact with the same or similar residues in the periplasmic and cytoplasmic sides of the transporter. However, other factors have to contribute to make the K_m at the outer site 10 times lower than the K_m for nonvectorial phosphorylation, as reported for EII^{Man} (*19*), EII^{GlcNAc} (*20*), and EII^{Mtl} (*36*).

The glucose-6-aldehydes do not follow this trend, at least in the case of EII^{Glc}. These nonphosphorylatable analogues are by far the strongest inhibitors of nonvectorial phosphorylation but comparatively weak inhibitors of uptake. Therefore, the reacting C-6 position appears to be an important determinant for binding from the periplasmic side of EII^{Glc}. Such a high specificity for the reactive OH-6 could be expected if the phosphoryl group on Cys421 of IICB^{Glc} were constitutive for the formation of the periplasmic binding site, for instance, as part of a hydrogen bond network between the active site and hydroxyl groups of the substrate.

Table 4: Classification of Glucose Analogues According to Effect on Phosphorylation and Uptake

properties[a,b]	sugar analogue: EII^{Glc}	sugar analogue: EII^{Man}
transport inhibition and phosphorylated nonlinearly	Glc	Glc
	α-1FGlc	1dGlc
	β-1FGlc	α-1FGlc
		β-1FGlc
transport inhibition and phosphorylated linearly		mannose
	1dGlc	2dGlc
	3FGlc	2FGlc
		3FGlc
no transport inhibition and phosphorylated linearly	mannose	
	2dGlc	
	2FGlc	allose
	allose	3dGlc
	3dGlc	
	4FGlc	
no transport inhibition and not phosphorylated	galactose	galactose
	4dGlc	4dGlc
	6dGlc	4FGlc
	6FGlc	6dGlc
		6FGlc

[a] An analogue is considered an inhibitor of transport when the rate of transport of [^{14}C]αMGlc or [^{14}C]2dGlc is reduced at least by half in the presence of a 10-fold excess of the analogue (see Figure 2). [b] Analogues for which V_{max}/K_m of EII^{Glc} or EII^{Man} are less than 2% of their V_{max}/K_m for glucose or mannose, respectively, are not considered pseudosubstrates (see Table 1).

Binding of the bulkier geminal diol of the glucose-6-aldehydes to this site might be hampered by the presence of the phosphoryl group.

Biphasic Eadie−Hofstee plots were obtained with glucose, and other substrates, in reactions catalyzed by EII^{Glc} and EII^{Man}. Similar kinetics have been reported for the mannitol PTS transporter (*4*, *37*). This kinetic behavior is probably a consequence of the presence of two independent phosphorylation activities associated with the transporter. Lolkema et al. proposed for EII^{Mtl} the coexistence of one vectorial and one nonvectorial activity in vitro (*37*). Nonvectorial activity would be caused by inside-out membrane vesicles and vectorial activity by a small fraction of open structures. Our data do not support such explanation. According to it, all analogues of glucose that are transported

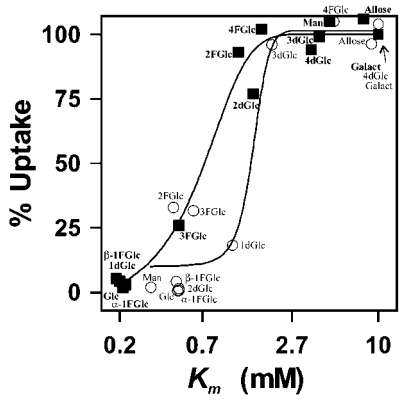

FIGURE 9: Correlation between efficacy of uptake inhibition and K_m in nonvectorial phosphorylation of pseudosubstrates. Plotted is the percent inhibition of uptake by these analogues (taken from Figure 2) versus the Michaelis constant of phosphorylation (K_m, taken from Table 1) for EII^{Glc} (solid squares) and EII^{Man} (open circles). The pseudosubstrates are indicated by abbreviated names, in bold face for EII^{Glc} and light face for EII^{Man}.

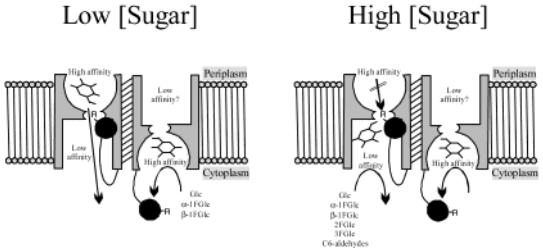

FIGURE 10: Working model for the $IICB^{Glc}$ dimer of EII^{Glc}. $IICB^{Glc}$ consists of a membrane-spanning C domain (gray) and the cytoplasmic IIB domain (black). Each B domain can functionally interact with each C domain in the dimer (*6*). $IICB^{Glc}$ is phosphorylated at Cys-421 by the soluble IIA^{Glc} subunit. It is proposed that two nonvectorial phosphorylation activities (curved arrows) are due to the presence of two cytoplasmically oriented binding sites per dimer, with different affinities for glucose. Other details are given in the text.

by EII would necessarily also display nonlinear phosphorylation kinetics. This is not the case, for instance, for 3FGlc (see Table 4).

On the basis of the kinetic data presented in this work, a working model of EII (Figure 10) with the following properties is proposed. (i) EIIs have two catalytic sites for nonvectorial phosphorylation per dimer, one high affinity and one low affinity, which are simultaneously accessible from the cytoplasmic side. That allows to explain the biphasic kinetics of nonvectorial phosphorylation. (ii) EIIs have one site which is accessible from the periplasmic site and has kinetic properties similar to, but not necessarily identical with, the cytoplasmic high-affinity site. A periplasmic low-affinity site could be postulated only for reasons of symmetry, for instance, assuming a reciprocally alternating conformation of the two subunits in the dimer. There is no experimental evidence, however, for that low-affinity site. When the raw data reported for transport experiments with EII^{Man} (*19*) and EII^{GlcNAc} (*20*) reconstituted in proteoliposomes are replotted in the Eadie−Hofstee form, the data points appear linearly distributed. If a low-affinity site existed, its catalytic efficiency is below the limit of detection. (iii) Substrate analogues such as 3FGlc and the nonphosphorylatable aldehydes preferentially interact with the cytoplasmic low-affinity site and therefore show simple kinetics. The high-affinity site seems to be less tolerant to structurally diverse substrates. (iv) The periplasmic high-affinity and cytoplasmic low-affinity sites are either two isomeric forms of a single site in rapid equilibrium or are two structures coexisting in the same subunit. By this proposition the previously observed inhibition of transport by nonvectorial phosphorylation of substrates present in saturating concentrations (*20*) can be rationalized. (v) At low intracellular glucose concentrations nonvectorial phosphorylation takes place at the high-affinity site (left side, Figure 10). A conformational change might be required to position the phosphoryl group close to the reactive OH-6 of the bound sugar. In contrast, the low-affinity site presents a ready-to-react phoshoryl group site (right side, Figure 10).

ACKNOWLEDGMENT

We are indebted to Prof. Malcom Page (Basilea Pharmaceuticals, Basel, Switzerland) for fruitful discussions on kinetics aspects and to Karin Flükiger for technical assistance.

SUPPORTING INFORMATION AVAILABLE

One figure showing Michaelis−Menten plots of phosphorylation of deoxy and fluoro analogues and epimers of D-glucose by EII^{Glc} or EII^{Man} and one table giving ^1H and ^{13}C NMR data from synthetic intermediates in the preparation of aldehydes **1a**−**f**. This material is available free of charge via the Internet at http://pubs.acs.org.

REFERENCES

1. Postma, P. W., Lengeler, J. W., and Jacobson, G. R. (1993) Phosphoenolpyruvate: carbohydrate phosphotransferase systems of bacteria, *Microbiol. Rev. 57*, 543−594.
2. Saier, M. H. J., Chauvaux, S., Deutscher, J., Reizer, J., and Ye, J. J. (1995) Protein phosphorylation and regulation of carbon metabolism in gram-negative versus gram-positive bacteria, *Trends Biochem. Sci. 20*, 267−271.
3. Hurley, J. H., Faber, H. R., Worthylake, D., Meadow, N. D., Roseman, S., Pettigrew, D. W., and Remington, S. J. (1993) Structure of the regulatory complex of *Escherichia coli* IIIGlc with glycerol kinase, *Science 259*, 673−677.
4. Boer, H., ten Hoeve-Duurkens, R. H., Schuurman-Wolters, G. K., Dijkstra, A., and Robillard, G. T. (1994) Expression, purification, and kinetic characterization of the mannitol transport domain of the phosphoenolpyruvate-dependent mannitol phosphotransferase system of *Escherichia coli*. Kinetic evidence that the E. coli mannitol transport protein is a functional dimer, *J. Biol. Chem. 269*, 17863−17871.
5. Erni, B. (1986) Glucose-specific permease of the bacterial phosphotransferase system: phosphorylation and oligomeric structure of the glucose-specific IIGlc-IIIGlc complex of *Salmonella typhimurium*, *Biochemistry 25*, 305−312.
6. Lanz, R., and Erni, B. (1998) The glucose transporter of the *Escherichia coli* phosphotransferase system. Mutant analysis of the invariant arginines, histidines, and domain linker, *J. Biol. Chem. 273*, 12239−12243.
7. van Montfort, B. A., Schuurman-Wolters, G. K., Duurkens, R. H., Mensen, R., Poolman, B., and Robillard, G. T. (2001) Cysteine cross-linking defines part of the dimer and B/C domain interface of the *Escherichia coli* mannitol permease, *J. Biol. Chem. 276*, 12756−12763.
8. Koning, R. I., Keegstra, W., Oostergetel, G. T., Schuurman-Wolters, G., Robillard, G. T., and Brisson, A. (1999) The 5 A projection structure of the transmembrane domain of the mannitol transporter enzyme II, *J. Mol. Biol. 287*, 845−851.
9. Lolkema, J. S., Dijkstra, D. S., Ten Hoeve-Duurkens, R. H., and Robillard, G. T. (1990) The membrane-bound domain of the phosphotransferase enzyme IImtl of *Escherichia coli* constitutes a mannitol translocating unit, *Biochemistry 29*, 10659−10663.

10. Hummel, U., Nuoffer, C., Zanolari, B., and Erni, B. (1992) A functional protein hybrid between the glucose transporter and the *N*-acetylglucosamine transporter of *Escherichia coli*, *Protein Sci. 1*, 356−362.
11. Bouma, C. L., Meadow, N. D., Stover, E. W., and Roseman, S. (1987) II−BGlc, a glucose receptor of the bacterial phosphotransferase system: molecular cloning of ptsG and purification of the receptor from an overproducing strain of *Escherichia coli*, *Proc. Natl. Acad. Sci. U.S.A. 84*, 930−934.
12. Erni, B., Zanolari, B., and Kocher, H. P. (1987) The mannose permease of *Escherichia coli* consists of three different proteins. Amino acid sequence and function in sugar transport, sugar phosphorylation, and penetration of phage lambda DNA, *J. Biol. Chem. 262*, 5238−5247.
13. Williams, N., Fox, D. K., Shea, C., and Roseman, S. (1986) Pel, the protein that permits lambda DNA penetration of *Escherichia coli*, is encoded by a gene in ptsM and is required for mannose utilization by the phosphotransferase system, *Proc. Natl. Acad. Sci. U.S.A. 83*, 8934−8938.
14. Robillard, G. T., and Broos, J. (1999) Structure/function studies on the bacterial carbohydrate transporters, enzymes II, of the phosphoenolpyruvate-dependent phosphotransferase system, *Biochim. Biophys. Acta 1422*, 73−104.
15. Buhr, A., and Erni, B. (1993) Membrane topology of the glucose transporter of *Escherichia coli*, *J. Biol. Chem. 268*, 11599−11603.
16. Huber, F., and Erni, B. (1996) Membrane topology of the mannose transporter of *Escherichia coli* K12, *Eur. J. Biochem. 239*, 810−817.
17. Nuoffer, C., Zanolari, B., and Erni, B. (1988) Glucose permease of *Escherichia coli*. The effect of cysteine to serine mutations on the function, stability, and regulation of transport and phosphorylation, *J. Biol. Chem. 263*, 6647−6655.
18. Thompson, J., and Chassy, B. M. (1985) Intracellular phosphorylation of glucose analogues via the phosphoenolpyruvate: mannose-phosphotransferase system in *Streptococcus lactis*, *J. Bacteriol. 162*, 224−234.
19. Mao, Q., Schunk, T., Flukiger, K., and Erni, B. (1995) Functional reconstitution of the purified mannose phosphotransferase system of *Escherichia coli* into phospholipid vesicles, *J. Biol. Chem. 270*, 5258−5265.
20. Mukhija, S., and Erni, B. (1996) Purification by Ni2+ affinity chromatography, and functional reconstitution of the transporter for *N*-acetylglucosamine of *Escherichia coli*, *J. Biol. Chem. 271*, 14819−14824.
21. Czernecki, S., Vijayakumaran, K., and Ville, G. (1986) Convenient synthesis of hex-1-enopyran-3-uloses: selective oxidation of allylic alcohols using pyridinium dichromate, *J. Org. Chem. 51*, 5472−5475.
22. Garcia-Alles, L. F., Flukiger, K., Hewel, J., Gutknecht, R., Siebold, C., Schurch, S., and Erni, B. (2002) Mechanism-based inhibition of enzyme I of the *Escherichia coli* phosphotransferase system: Cys502 is an essential residue, *J. Biol. Chem. 277*, 6934−6942.
23. Buhr, A., Fluekiger, K., and Erni, B. (1994) The glucose transporter of *Escherichia coli*. Overexpression, purification, and characterization of functional domains, *J. Biol. Chem. 269*, 23437−23443.
24. Esquinas-Rychen, M., and Erni, B. (2001) Facilitation of bacteriophage lambda DNA injection by inner membrane proteins of the bacterial phosphoenolpyruvate: carbohydrate phosphotransferase system (PTS), *J. Mol. Microbiol. Biotechnol. 3*, 361−370.
25. Erni, B., and Zanolari, B. (1985) The mannose-permease of the bacterial phosphotransferase system. Gene cloning and purification of the enzyme IIMan/IIIMan complex of *Escherichia coli*, *J. Biol. Chem. 260*, 15495−15503.
26. Buhr, A., Daniels, G. A., and Erni, B. (1992) The glucose transporter of *Escherichia coli*. Mutants with impaired translocation activity that retain phosphorylation activity, *J. Biol. Chem. 267*, 3847−3851.
27. Kuzmic, P. (1996) Program DYNAFIT for the analysis of enzyme kinetic data: application to HIV proteinase, *Anal. Biochem. 237*, 260−273.
28. Mahrwald, R., Theil, F., Schick, H., Schwarz, S., Palme, H. J., and Weber, G. (1986) The oxidation of primary trimethylsilyl ethers to aldehydes − a selective conversion of a primary hydroxy group into an aldehyde group in the presence of a secondary hydroxy group, *J. Prakt. Chem. 328*, 777−783.
29. Koester, R., Idelmann, P., and Dahlhoff, W. V. (1982) Organoboron monosaccharides. XII. Quantitative preparation of D-glucohexodialdose from sodium D-glucuronate or D-glucuronic acid, *Synthesis*, 650−652.
30. Singh, S., Nambiar, S., Porter, R. A., Sander, T. L., Taylor, K. G., and Doyle, R. J. (1989) Dialdosides-(1,5) of glucose and galactose: synthesis, reactivity, and conformation, *J. Org. Chem. 54*, 2300−2307.
31. Beving, H. F. G., and Theander, O. (1975) Degradation of methyl α-D-glucohexo-1,5-dialdopyranoside in aqueous solution, *Acta Chem. Scand., Ser. B 29*, 577−581.
32. Hayashi, S. I., and Lin, E. C. (1967) Purification and properties of glycerol kinase from *Escherichia coli*, *J. Biol. Chem. 242*, 1030−1035.
33. Rendina, A. R., and Cleland, W. W. (1984) Mechanisms of aldehyde-induced adenosinetriphosphatase activities of kinases, *Biochemistry 23*, 5157−5168.
34. Haddad, J., Vakulenko, S., and Mobashery, S. (1999) An Antibiotic Cloaked by Its Own Resistance Enzyme, *J. Am. Chem. Soc. 121*, 11922−11923.
35. Segel, I. H. (1993) in *Enzyme Kinetics: Behavior and Analysis of Rapid Equilibrium and Steady-State Enzyme Kinetics*, Wiley & Sons, New York.
36. Elferink, M. G., Driessen, A. J., and Robillard, G. T. (1990) Functional reconstitution of the purified phosphoenolpyruvate-dependent mannitol-specific transport system of *Escherichia coli* in phospholipid vesicles: coupling between transport and phosphorylation, *J. Bacteriol. 172*, 7119−7125.
37. Lolkema, J. S., ten Hoeve-Duurkens, R. H., and Robillard, G. T. (1993) Steady-state kinetics of mannitol phosphorylation catalyzed by enzyme IImtl of the *Escherichia coli* phosphoenolpyruvate-dependent phosphotransferase system, *J. Biol. Chem. 268*, 17844−17849.

BI025928D